

S. M. Carbotte · R. E. Bell · W. B. F. Ryan
C. McHugh · A. Slagle · F. Nitsche · J. Rubenstone

Environmental change and oyster colonization within the Hudson River estuary linked to Holocene climate

Received: 18 September 2003 / Accepted: 13 April 2004 / Published online: 28 May 2004
© Springer-Verlag 2004

Abstract Geophysical mapping and sampling data provide a record of changing environmental and faunal conditions within the Hudson River estuary during the mid- to late Holocene. On the shallow, broad marginal flats of the mesohaline Hudson, fossil oyster beds (*Crassostrea virginica*) are found exposed on the river bottom and buried by sediment. The shallowest beds are well imaged in chirp sub-bottom and side-scan sonar data and form discrete flow-perpendicular bands, 0.6–1.0 km wide and up to 3 km long, which cover 30% of the river bottom. Radiocarbon-dated sediment cores indicate oysters thrived within two time periods from ~500–2,400 and ~5,600–6,100 cal. years B.P. Sediment and physical property data indicate a changing depositional regime consistent with the oyster chronology. Similar changes in oyster presence are found in local shell midden sites of the Lower Hudson Valley as well as elsewhere along the Atlantic coast, and may reflect climatic controls associated with warm–cool cycles during the Holocene. Oysters flourished during the mid-Holocene warm period, disappeared with the onset of cooler climate at 4,000–5,000 cal. years B.P., and returned during warmer conditions of the late Holocene. The most recent demise of oysters within the Hudson at 500–900 cal. years B.P. may have accompanied the Little Ice Age.

Introduction

Humans have long settled estuary banks where food resources are abundant and accessible routes for transportation and trade are present. As estuaries emerged as favored sites for urban development and industrialization within the past two centuries, widespread degradation of estuarine ecosystems occurred. Although the modern collapse of coastal ecosystems is widely attributed to anthropogenic factors (e.g., Jackson et al. 2001), these ecosystems are also vulnerable to environmental transformation associated with sea-level rise and climate change (Walther et al. 2002).

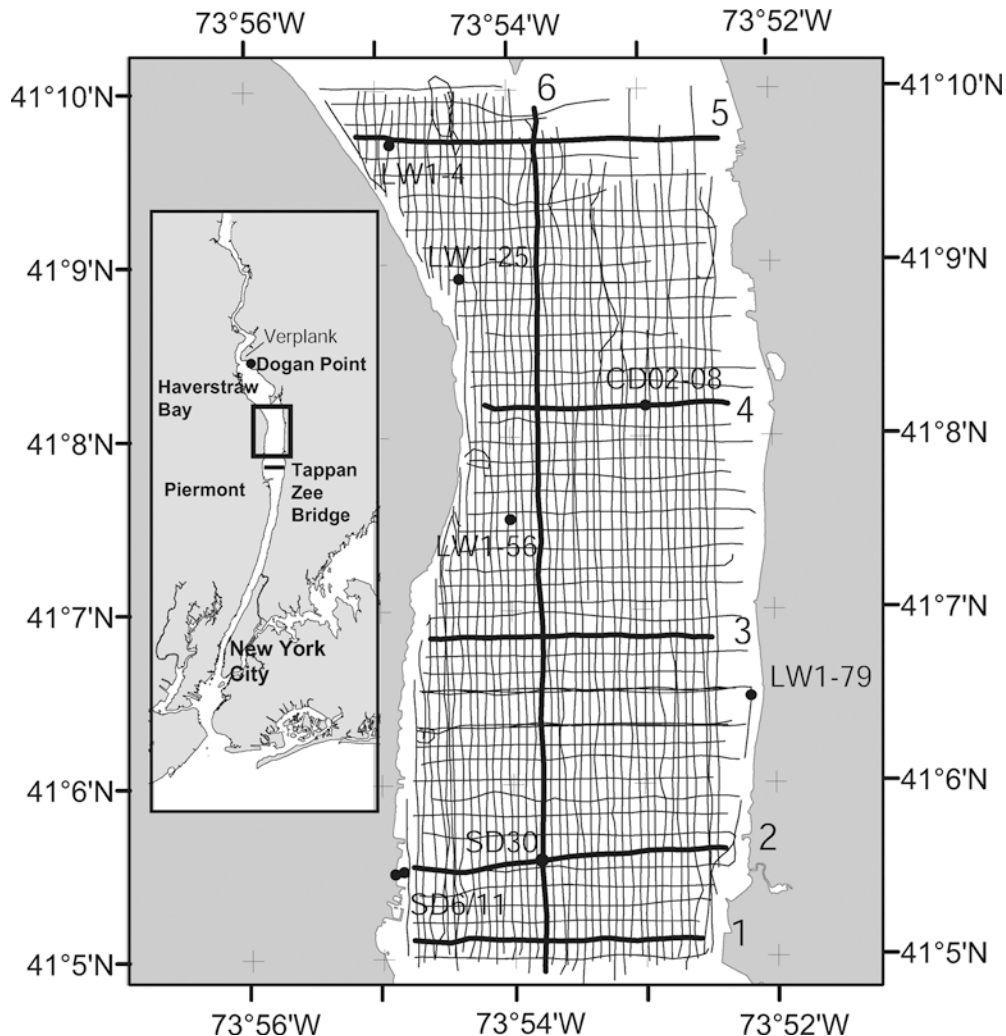
Within the Hudson River estuary, oysters were once an abundant estuarine resource, as evidenced by the presence of numerous prehistoric oyster shell middens (mounds of discarded shells) left along the shores of the Hudson by indigenous peoples. The earliest record of marine shellfishing anywhere along the western Atlantic coast is at Dogan Point on the eastern Hudson shore south of Verplanck, where oyster harvesting began ~6,000 cal. years B.P. (e.g., Brennan 1974; Claassen 1995, Fig. 1). The Dogan Point shell middens contain two distinct shell layers. At the base of the middens are “giant” oyster (GO) shells 10–13 cm long, dating to 5,100–5,900 cal. years B.P. (Brennan 1974; Little 1995; see Radiocarbon age dating section below). Above this horizon is a younger, small oyster (SO) horizon with 7–8 cm valve lengths. Shells from the SO horizon form two age groups (4,000–5,100 and 1,500–1,800 cal. years B.P.) separated by a distinct hiatus of roughly 2,000 years. Archeologists have debated whether the oyster hiatus revealed in the shell matrix sites of the lower Hudson reflects change in the estuarine environment or anthropogenic factors such as over-exploitation, a change in dietary preferences or migration patterns of the resident indigenous peoples (e.g., Schuldenrein 1995; Claassen, 1995).

In this study we present evidence from new geophysical and sampling data for fossil oyster beds within

S. M. Carbotte (✉) · R. E. Bell · W. B. F. Ryan · C. McHugh
A. Slagle · F. Nitsche · J. Rubenstone
Lamont-Doherty Earth Observatory of Columbia University,
Box 1000, Palisades, NY, 10964, USA
E-mail: carbotte@ldeo.columbia.edu
Tel.: +1-845-3658895
Fax: +1-845-3653181

C. McHugh
Queens College, CUNY, Flushing, NY, 11367, USA

Fig. 1 Side-scan sonar and chirp sub-bottom track coverage within the Tappan Zee study area. Numbered tracks (1–6) correspond with chirp profiles shown in Figs. 3 and 4. Locations of gravity and vibrocores used in this study are also indicated, along with core numbers. Inset shows location of study area (rectangle) along the Hudson River estuary, with key geographic features referred to in the text



the mesohaline Hudson River estuary, with ages that are consistent with the shell chronology found in local middens. The data include a dense grid of high-resolution side-scan sonar imagery and chirp sub-bottom profiles as well as a suite of sediment cores. Geophysical data are used to define the spatial distribution and geometry of the oyster beds. Radiocarbon-dated sediment cores are used to characterize environmental conditions during the periods of oyster growth and to define the local depositional regime. The data indicate that changing environmental conditions rather than anthropogenic effects account for the oyster hiatus observed within the Hudson Valley shell middens. We discuss possible factors that may have contributed to the observed changes in faunal and sedimentary conditions within the estuary, including the role of sea-level rise and climate.

Materials and methods

In fall of 1998, a major geophysical mapping and sampling effort within the Hudson River estuary was

initiated by the New York State Department of Environmental Conservation. The goal of the project was to provide high-resolution baseline characterization of the river bottom for studies of benthic habitats and sediment transport. As part of this program, side-scan sonar, chirp sub-bottom, single and multibeam bathymetry data, as well as an extensive suite of sediment core and grab samples have been acquired by researchers at Lamont-Doherty Earth Observatory, SUNY Stony Brook and Queens College (Bell et al. 2000, 2003). Data collection occurred during five field seasons spanning 1998 to 2003, and provides shore-to-shore coverage for much of the river from the New York Harbor to the Troy Dam.

Here we focus on data collected within a five-mile stretch of the river located north of the Tappan Zee Bridge (Fig. 1). Side-scan sonar data were acquired along an orthogonal grid of 85-m-spaced north-south lines and 165-m-spaced east-west lines, using a dual-frequency (100 and 384 kHz) Edgetech sonar (Figs. 1 and 2). An Edgetech 4–24 kHz chirp sonar and XSTAR acquisition unit were used to collect high-frequency subbottom data (Schock and Leblanc 1990) simultaneously

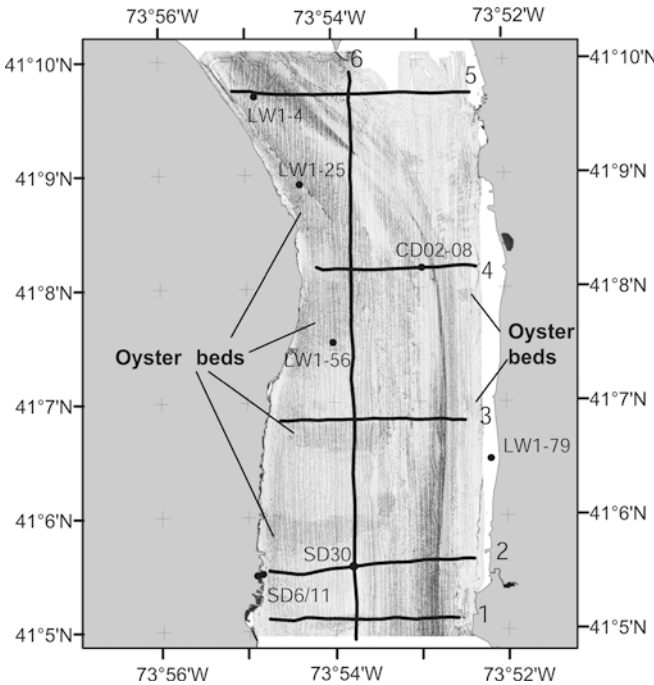


Fig. 2 Side-scan sonar mosaic (100 kHz) acquired along north-south tracks shown in Fig. 1. Numbered tracks (1–6) correspond with chirp profiles shown in Figs. 3 and 4. Locations of gravity and vibrocores used in this study are shown along with core numbers. General areas of moderate backscatter, which correspond with oyster beds exposed on river bottom, are indicated

with the side-scan operations. The chirp data were collected at a shot rate of 5 per second, with tow speeds ranging from 4 to 5.5 knots. A swept frequency range of 4–16 kHz was used, providing a practical vertical resolution of 5–10 cm. Geophysical data were layback-corrected to account for offsets between the position of the towed sensors and the GPS antennae. Final positional uncertainties of ~1 m were obtained by post-processed differential pseudo-range GPS. Chirp data were gain-adjusted. A constant correction for tow fish depth of 1.3 m was applied, estimated from average travel time difference between the water bottom return and first water bottom multiple. Under normal, underway operations, fish depth variations were typically less than 0.33 m. Corrections for tidal fluctuations were also applied, using tidal records from locally installed gauges. Tide-corrected data were then loaded into the Geoquest seismic interpretation package for identification and mapping of sub-bottom horizons.

A suite of shallow (up to two-meter) gravity cores (LW1-4, LW1-25, LW1-56, LW1-79) and four 8–10 m long vibrocores (SD6, SD11, SD30, CD02-08) provide information on sediment properties and shell material for age dating (cf. Fig. 1 and Table 1 for core locations). The primary cores used in this study are vibrocores SD30, located near the western margin of the main channel, and SD11 located near shore. Core SD11 was collected as part of a dense near-shore cluster (which also included SD6) targeted for environmental assess-

ment objectives. Core SD30 was sited to sample horizons within the sub-bottom data, including a shallow reflection believed to be an oyster shell layer of limited lateral and vertical extent where good core penetration was expected. Physical properties were measured using a GEOTEK multi-sensor core logger and include compressional (P-wave) velocity, magnetic susceptibility, and sediment bulk density via gamma ray attenuation. Cores were split and photographed, and are archived at the Lamont-Doherty Earth Observatory Deep Sea Sample Repository. Bottom photography, acquired with a sediment profile imagery (SPI) system, provides information on sediments and benthic fauna at the sediment/water interface along several east–west transects of the river (NOAA 2000).

Radiocarbon age dating

Radiocarbon ages were obtained for individual shells sampled from our cores by accelerator mass spectrometry (AMS). Details on the dated shells, including core identification numbers, sample material and depths, radiocarbon laboratory, and ^{14}C age, are given in Table 2. The measured dates are calibrated to calendar years using CALIB 4.3 (Stuvier et al. 1998, 2001), after applying a reservoir correction of 950 years derived from three pre-bomb shells collected within the region (J. Rubenstein and D. Peteet, personal communication). To obtain a consistent chronology for river and midden shells, we apply this same reservoir correction to the radiocarbon ages for the Dogan Point shells reported by Little (1995). The Hudson correction is larger than the standard marine correction of ~400 years, and indicates the presence of old terrestrial carbon, possibly derived from erosion of Paleozoic limestones located along the Hudson north of Wappinger Falls and/or soil erosion from the Hudson watershed. For comparison, the reservoir correction for Chesapeake Bay determined from similar pre-bomb shell dating is 365 ± 143 years, which is not significantly different from the standard marine correction and indicates little contribution of old carbon in this reservoir (Colman et al. 2002).

Results

The geophysical and sampling data reveal fossil oyster beds on the Hudson River bottom from Piermont to Haverstraw Bay (Fig. 1). Within the Tappan Zee region, located ~10 km south of the Dogan Point shell midden site, oyster beds coincide with discrete bands of moderate backscatter that extend across the marginal flats (Fig. 2). The marginal flats border the main channel (Fig. 3) and lie at a near-constant depth of 4.0–4.5 m (referenced to NAVD88), with portions of exposed oyster beds elevated slightly (30–90 cm) above the surrounding river bottom (Fig. 4).

Table 1 Locations of sediment cores in the Tappan Zee study area

| Core number ^a | Latitude (N) | Longitude (W) | Water depth ^b (cm) | Date of collection | Core type | Core diameter (inch) |
|--------------------------|--------------|---------------|-------------------------------|--------------------|-----------|----------------------|
| SD30 | 41°05.5625' | 73°53.8054' | 436 | Dec. 1999 | Vibracore | 4 |
| SD11 | 41°05.47122' | 73°54.83442' | 204 | Dec. 1999 | Vibracore | 4 |
| SD6 | 41°05.47007' | 73°54.87997' | 105 | Dec. 1999 | Vibracore | 4 |
| LW1-79 | 41°06.5140' | 73°52.18998' | 372 | June 1999 | Gravity | 4 |
| LW1-25 | 41°08.8860' | 73°54.3990' | 473 | June 1999 | Gravity | 4 |
| LW1-56 | 41°07.5240' | 73°54.00102' | 440 | June 1999 | Gravity | 4 |
| LW1-4 | 41°09.690' | 73°54.8820' | 1,091 | June 1999 | Gravity | 4 |
| CD02-08 | 41°08.17674' | 73°52.96824' | 958 | June 2002 | Vibracore | 4 |

^aCores are curated and stored within the Lamont-Doherty Earth Observatory Deep-Sea Sample Repository^bWater depth below mean sea level referenced to NAVD88**Table 2** Radiocarbon ages of bivalve shells in the Tappan Zee study area

| Core number | Sample depth ^a (cm) | Material ^b | Laboratory ^c | $\delta^{13}\text{C}$ ^d (‰) | Age ^e (^{14}C years) | Error ^e (years) | Calibrated age (min., max.) ^f (cal. years B.P.) |
|-------------|--------------------------------|-----------------------|-------------------------|--|---|----------------------------|--|
| SD30 | 8 | CV | NOSAMS | -5.83 | 1,940 | 35 | 927 (793, 963) |
| | 75 | CV | Zurich | 2.2 | 2,370 | 60 | 1,307 (1,260, 1,413) |
| | 202 | Bivalve | NOSAMS | -2.13 | 3,720 | 50 | 2,853 (2,763, 2,965) |
| | 284 | Bivalve | NOSAMS | -3.14 | 4,160 | 35 | 3,425 (3,359, 3,544) |
| | 530 | Bivalve | NOSAMS | -2.40 | 4,800 | 65 | 4,244 (4,019, 4,422) |
| | 574 | Bivalve | NOSAMS | -2.53 | 4,820 | 65 | 4,287 (4,090, 4,502) |
| | 695 | Bivalve | NOSAMS | -2.68 | 5,060 | 40 | 4,608 (4,447, 4,824) |
| | 727 | Bivalve | NOSAMS | -1.82 | 5,250 | 65 | 4,851 (4,654, 5,035) |
| | 850 | Bivalve | NOSAMS | -2.69 | 6,150 | 65 | 5,931 (5,755, 6,172) |
| | 925 | CV | Zurich | 2.3 | 6,270 | 70 | 6,058 (5,926, 6,284) |
| | 158 | CV | LLNL | 0 | 2,560 | 35 | 1,522 (1,411, 1,585) |
| SD11 | 314 | Bivalve | LLNL | 0 | 4,230 | 40 | 3,473 (3,397, 3,631) |
| | 760 | Bivalve | LLNL | 0 | 6,295 | 45 | 6,133 (5,952, 6,277) |
| LW1-79 | 160 | CV | Zurich | 0.2 | 3,050 | 60 | 2,091 (1,902, 2,305) |
| LW1-25 | 15 | CV | Zurich | -2.2 | 1,765 | 55 | 728 (660, 906) |
| LW1-56 | 95 | CV | Zurich | -0.2 | 3,280 | 65 | 2,346 (2,155, 2,706) |
| LW1-4 | 105 | CV | Zurich | 1.5 | 2,135 | 60 | 1,164 (961, 1,264) |
| CD02-08 | 273 | CV | LLNL | -2.5 | 2,080 | 40 | 1,028 (952, 1,170) |

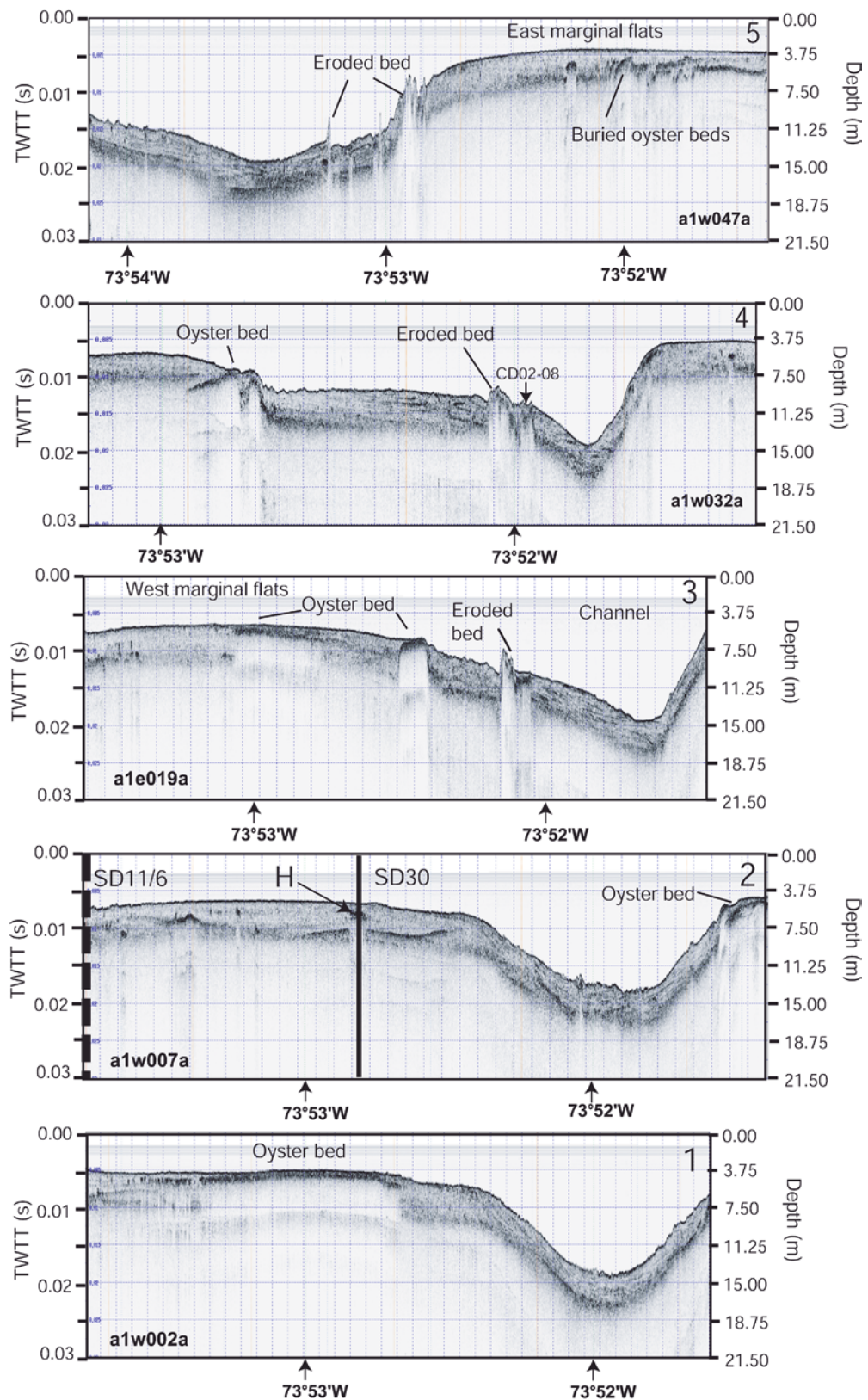
^aSample depth is within core^bCV, *Crassostrea virginica*^cLNLL, Lawrence Livermore National Labs; NOSAMS, National Ocean Science Accelerator Mass Spectrometry facility at Woods Hole Oceanographic Institute; Zurich Radiocarbon Laboratory, University of Zurich^d $\delta^{13}\text{C}$ values of 0 assumed; all others measured^eOne sigma^fRadiocarbon ages are calibrated to calendar years using CALIB 4.3 (Stuiver et al. 1998, 2001), after applying a reservoir correction of 950 years obtained from pre-bomb shells within the study area (J. Rubenstein and D. Peteet, unpublished data)

In the sub-bottom data, oyster beds appear as bright, acoustically impenetrable reflections coincident with the moderate backscatter regions in the side-scan sonar data but also buried by up to 3 m of sediment (Figs. 3 and 4). Oyster beds extend as continuous structures into the subsurface and typically dip gently to the north, with a steep scarp at their southern edge (Figs. 3 and 4). Individual oyster beds are ~0.6–1 km wide and up to 3 km long but may have once reached from bank to bank (Fig. 5). Isolated protrusions with oyster shell layers are present within the channel bank sediments, which appear to be erosional remnants of beds formerly continuous with those of the marginal flats (Figs. 3, 4 and 5). These isolated structures are always lower in elevation than oyster beds on the nearby marginal flats, consistent with an erosional formation. The oyster beds imaged with the geophysical data cover ~30% of the estuary floor within the Tappan Zee (Fig. 5). Sub-bottom penetration

throughout the region is limited to ~4 m below river bottom, presumably due to gas presence within the sediments (e.g., Hagen and Vogt 1999). However, vibracores reveal deeper oyster shell layers, 6.5–9.5 m below river bottom.

The shells belong exclusively to the eastern oyster species *Crassostrea virginica* (Gmelin 1791). Although salinities within this stretch of the Hudson (summer range of ~10–13 ppt) are adequate to support living specimens, these are rare in grab samples and bottom photographs and always small, presumably juvenile specimens. Radiocarbon data indicate that the Hudson River oyster shells lie within two age brackets consistent with the Dogan Point shell middens (Table 2, Figs. 5 and 6). Shells from the upper parts of the cores have ages of 520–2,346 cal. years B.P. whereas those from the lower parts were deposited 5,660–6,058 cal. years B.P. In between is a layer of sediment 3–6 m thick without oyster shells. As is the case for the middens, shells from the

Fig. 3 East-west-oriented chirp sub-bottom profiles (1–5) showing oyster bed horizons and other sub-bottom reflections. Oyster beds are imaged exposed on the river bottom (profiles 1 and 3) and buried in the shallow subsurface (profiles 1–5). Isolated elevated structures within the channel bank sediments are found (profiles 3–5), which may be erosional remnants of oyster beds formerly continuous with those of the marginal flats. Cores SD30 and SD11/6 intersect profile 2 at the locations indicated by bold line (cores SD11 and SD6, indicated by dashed bold line, are 200 and 250 m SW of the profile). Due to anticipated difficulties in achieving core penetration through oyster shell layers, core SD30 was located through a seismic horizon (H , profile 2) suspected to be a shell layer of limited lateral and vertical extent (see also profile 6, Fig. 4). Oyster shells were found within the core at the depth predicted from the sub-bottom data as well as deeper in the core, below the limit of acoustic penetration (Fig. 6, see text). Core CD02-08 was located to sample one of the elevated structures found within the channel bank sediments (profile 4). Oyster shell layers recovered within this core confirm that this structure coincides with an oyster bed



base of the cores are larger (10 cm) than the shallower shells (7–8 cm). The intervening layer of oyster-free sediment is consistent with the hiatus inferred from the

midden ages. The combined river-midden dataset suggests the oyster hiatus lasted from ~2,500 to 4,000 years B.P. within the region.

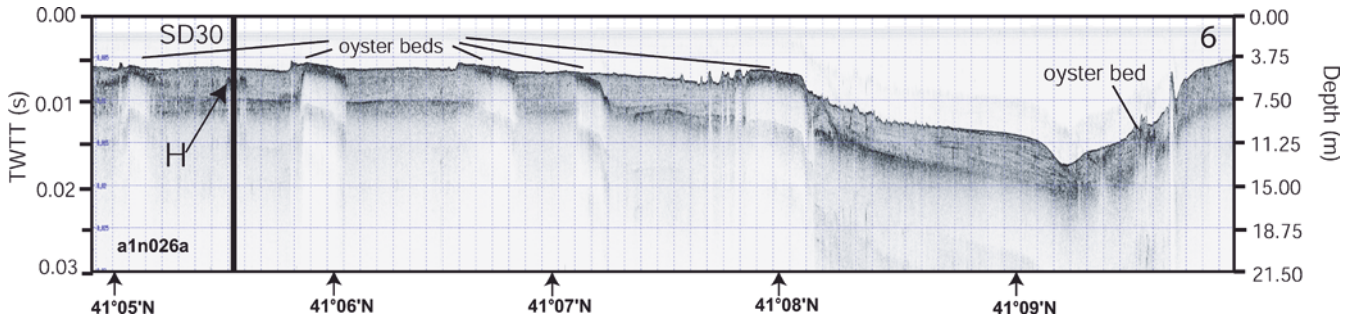


Fig. 4 North-south-oriented chirp sub-bottom profile 6 showing oyster bed horizons. Oyster beds form narrow bands, ~600–1,000 m wide, which rise 30–90 cm above surrounding river bottom, typically along their southern edge, and extend roughly east–west across the marginal flats. Core SD30 intersects profile 6 at the location indicated by the bold line. *H* Seismic horizon

Our cores contain three distinct lithofacies linked to the oyster chronology (data for cores SD30 and SD11 shown in Fig. 6). The oldest, lithofacies 3, is comprised of sparsely laminated clayey silts with scattered, large oyster shells. At near-shore sites (SD6), lithofacies 3 directly overlies reddish sand, which is likely of post-glacial fluvial origin (Newman et al. 1969). Lithofacies 3

Fig. 5 Side-scan sonar mosaic with locations of oyster beds (*Crassostrea virginica*) mapped from geophysical data delineated. Oyster beds exposed on the river bottom or buried by up to a few centimeters of sediment (approximate depth penetration of 100-kHz sonar) are detected in the side-scan imagery and are shown in darker blue. Beds buried in the shallow subsurface as mapped from chirp sub-bottom data are shown in light blue. Red dots show locations of cores with dated oyster shells. Ages of oysters are given in cal. years B.P. (Table 2; cf. Fig. 1 and Table 1 for core identification numbers); asterisks denote dates from McHugh et al. (2004) and Pekar et al. (2004). Shells chosen for radiocarbon dating are primarily from in-situ oyster beds as interpreted from the sub-bottom data. Bold black lines mark boundary between marginal flats and channel. Track lines for the chirp profiles in Figs. 3 and 4 are shown as thin blue lines. Locations of sediment profile imagery (SPI) data where oyster shells were observed on the river bottom are from NOAA (2000)

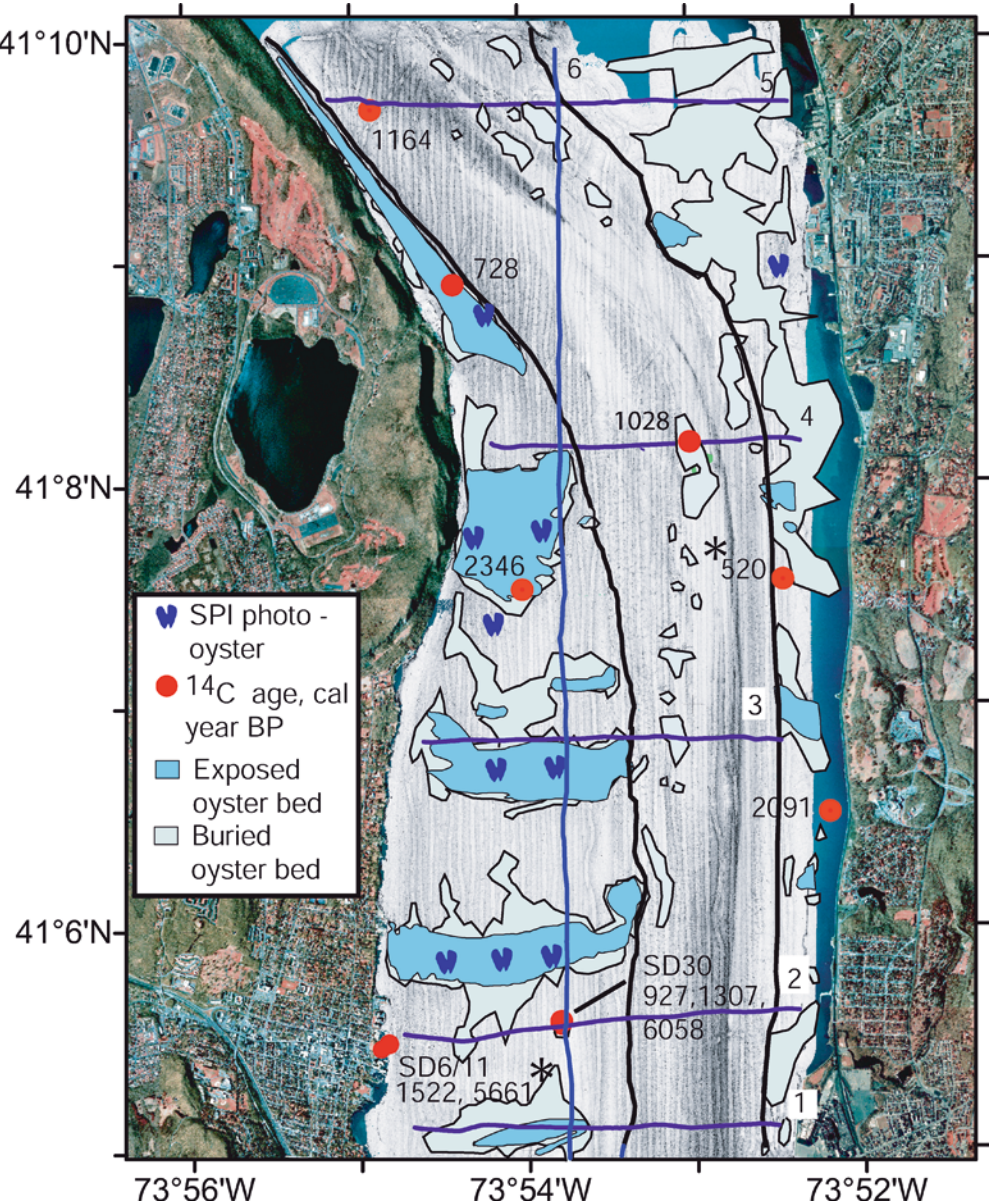
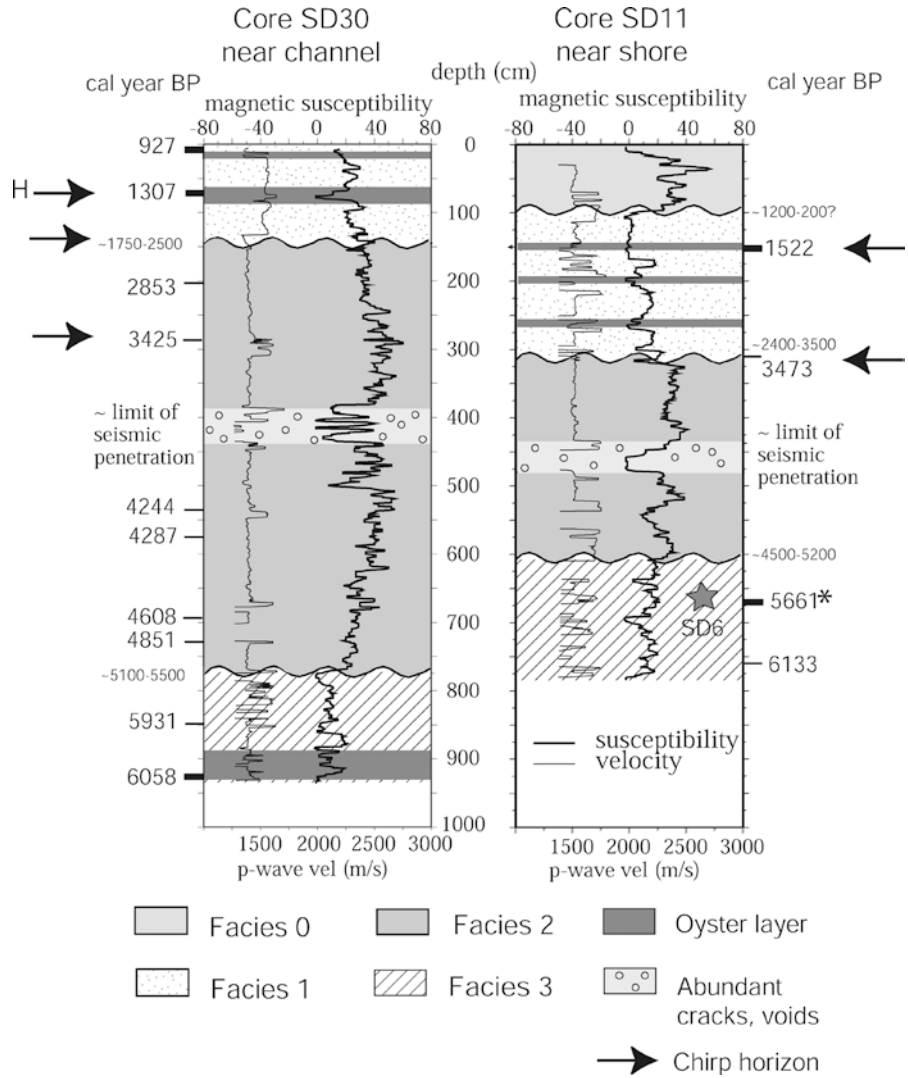


Fig. 6 Lithofacies in cores SD30 and SD11 and physical properties. Darkly shaded bands indicate oyster shell layers, facies are described in the text. Abrupt changes in magnetic susceptibility and P-wave velocity accompany facies transitions. Calendar ages are from individual shells (thick line for oysters, thin line for other bivalves, Table 2). The star denotes the depth of large oyster shells found in core SD6 (~50 m southeast of core SD11), which overlies a lithologic transition to fluvial sands (asterisk denotes age from Pekar et al. 2004). Wavy lines indicate possible unconformities, with estimated duration of unconformities also shown (see text). H denotes depths to seismic horizon identified on chirp profiles 2 and 6 (Figs. 3 and 4). Two-way travel time to depth conversion is carried out assuming a constant velocity of 1,500 m/s



has intermittently high P-wave velocities as well as frequent intervals of high acoustic attenuation, due to abundant cracks and voids (Fig. 6). We attribute these cracks and voids to sediment degassing on core extraction, and use variations in acoustic attenuation within our cores as a proxy indicator of relative variations in sediment gas concentrations. We emphasize that with gas-charged sediments, the P-wave velocities we measure on unpressurized cores in the laboratory will not reflect in-situ seismic velocities, and can not be used to convert two-way travel times to seismic horizons to depth.

Lithofacies 2 is composed of alternating laminated and massive clayey silts with frequent shelly layers (10–30 cm thick) of small, thin-walled bivalves (predominantly *Mulinia Lateralis*), but a notable lack of oyster shell. Higher magnetic susceptibilities characterize this lithofacies, indicating increased abundance of magnetic minerals. A localized zone of high acoustic attenuation and abundant voids, indicating sediments with higher gas concentrations, are observed in both SD11 and SD30 in the middle of lithofacies 2, at a depth of 4–4.5 m. This depth interval coincides well with the

approximate limit of seismic penetration throughout the region. The gas present within these sediments prior to core extraction is likely biogenic methane created by long-term chemical decomposition processes within buried sediments with high organic contents (e.g., Hill et al. 1992; Hagen and Vogt 1999).

Lithofacies 1 in the upper part of our cores (Fig. 6) corresponds again with sparsely laminated clayey silts with oyster shell layers similar to lithofacies 3. Lithofacies 1 has higher P-wave velocities and lower magnetic susceptibility than lithofacies 2. The available age control indicates low sedimentation rates of ~1–2 mm/year for both lithofacies 1 and 3, with higher rates of 2–4 mm/year for lithofacies 2.

The contacts between the lithofacies are visually distinct and accompanied by abrupt changes in physical properties (Fig. 6), suggestive of erosion or periods of non-deposition. From linear extrapolation of sedimentation rates derived for each facies, we estimate the possible time intervals represented by these unconformities to be ~1,750–2,500 and 5,100–5,500 years B.P. within SD30, and 2,400–3,500 and 4,500–5,200 years B.P.

within SD11 (Fig. 6). Although these estimates are subject to large uncertainties due to the sparse age control, they suggest that unconformities of greater duration are present in the near-shore core SD11 than in the near-channel core SD30 (by few 100s of years).

The uppermost one meter of sediment in the near-shore core SD11 is composed of water-saturated clayey silts and does not contain oysters (lithofacies 0). Anthropogenic detritus including slag and brick dust is found in these sediments, and may account for the exceptionally high magnetic susceptibilities measured. This facies, which is not found in SD30, appears to correspond with the recently deposited sediments found within the region in localized zones along the shoreline (Bell et al. 2000; McHugh et al. 2004).

Paleowater depths for our core locations are estimated using the relative sea-level curve for the Hudson River derived from the Peltier (1998) model for post-glacial isostatic adjustment (Fig. 7). This model fits the sparse existing sea-level observations from the Hudson well (Peltier 1999), and indicates gradual sea-level rise throughout the mid- to late Holocene. Estimated paleowater depths at the near-channel SD30 site are ~6 m during deposition of lithofacies 3. Depths rapidly shoal from 6 to 4 m with deposition of lithofacies 2, and re-

main near-constant at ~4 m during deposition of lithofacies 1. Paleowater depths at the near-shore core SD11 site have remained close to modern depths of ~2 m throughout this time.

Discussion

Depositional history within the Tappan Zee study area

The three lithofacies observed across the marginal flats of the Tappan Zee indicate a changing depositional regime over the past 6,100 cal. years B.P. Within our cores, the oldest lithofacies is found in direct contact with fluvial sands at the near-shore sites, and we attribute this facies to deposition in a restricted, marginal estuarine setting following marine incursion into the Tappan Zee region prior to 6,100 cal. years B.P. Similar restricted-estuarine sediments with oyster layers occur above the fluvial-estuarine contact within the northern Chesapeake Bay, and are credited to flooding of the banks of the paleo-Susquehanna River at 7,000–8,000 cal. years B.P. (Bratton et al. 2003). The more rapidly accumulating, alternating massive and laminated sediments of lithofacies 2 are similar to the open estuarine muds of Chesapeake Bay (e.g., Baucom et al. 2001), and coincide with the absence of oysters. Infilling of accommodation space on the marginal flats in response to rising sea level (e.g., Olson et al. 1978; McHugh et al. 2004), possibly due to sediment trapping at a migrating paleo-estuarine turbidity maximum (Pekar et al. 2004), may explain this phase of more rapid sedimentation and shoaling paleowater depths (Fig. 7).

Oysters return during the deposition of lithofacies 1. Estimates of paleowater depths at both core locations (Fig. 7) indicate sedimentation kept pace with rising sea level at rates of 1–2 mm/year during deposition of lithofacies 1. We attribute the sparsely laminated sediments and low deposition rates compared with lithofacies 2 to a depositional regime limited by benthic wave activity. Bottom sediment resuspension due to wind-generated wave activity is documented in shallow regions of Chesapeake Bay (3.5–5.5 m; Sanford 1994), and may be a significant process within the broad Tappan Zee where there is a long open fetch and similarly shallow water depths (< 4.5 m).

The modern environment on the marginal flats is dominated by non-deposition or erosion presumably maintained by benthic wave activity. With the exception of a now-filled 19th century channel into Nyack, New York, and local accumulations within sheltered embayments along the shoreline, radioisotope and sediment studies indicate that modern (post-1957) sediments are not accumulating on the marginal flats (Bell et al. 2000; McHugh et al. 2004). Indeed, existing age constraints indicate the youngest sediments on the marginal flats date to > 500 cal. years B.P. (Fig. 5). The near-horizontal surface of the marginal flats at present, with subtly

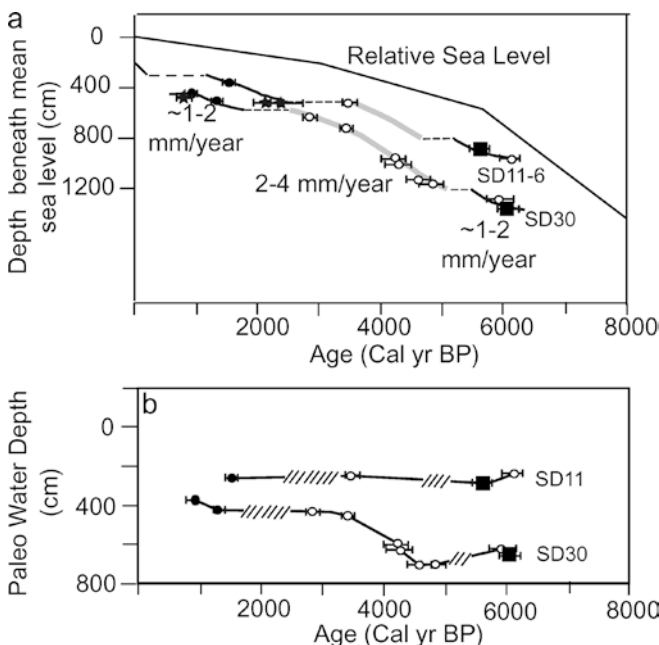


Fig. 7 **a** Age-depth data for Hudson River cores (Table 2), with sedimentation rates indicated. Symbols show control points; closed symbols correspond with oyster shell (circles small oyster shells, squares large oyster shells, stars oyster shells from other cores located elsewhere on marginal flats at similar water depths, see Fig. 5); open circles denote other bivalves. Solid bold and shaded lines on age-depth curves denote sediment lithofacies from Fig. 6, with interpolated time intervals associated with unconformities at facies boundaries in dashed line. Water depths are referenced to NAVD88 (~mean sea level). Solid bold lines show relative sea-level curve for the Hudson River from Peltier (1998). **b** Paleowater depths at cores SD30 and SD11. Time intervals associated with unconformities are shown with hatched lines

elevated oyster beds, is indicative of the erosive effects of benthic wave activity that leaves resistant oyster beds higher than the surrounding mud bottom. Erosive activity is also evident in the isolated oyster bed structures found within the sediments bounding the main channel, which appear to be remnants of beds formerly continuous with those of the marginal flats. Similar isolated features with oyster shells are also found within the Chesapeake Bay, where they are attributed to erosion of larger beds by wave cutting (Smith et al. 2003).

The inferred ages of unconformities marking the facies transitions in our cores overlap in time (~1,750–2,500 and 2,400–3,500 cal. years B.P. for the facies 1/2 transition, and 5,100–5,500 and 4,500–5,200 cal. years B.P. for the facies 2/3 transition within SD30 and SD11, respectively, Fig. 6), and indicate two periods of non-deposition or erosion across the marginal flats. Core SD11 is located only 80 m from the modern shoreline, and we attribute the greater duration of unconformities marking facies boundaries in this core to enhanced wave-driven erosion at the shoreline.

The two interruptions in sedimentation across the marginal flats could be the consequence of reductions in sediment supply from the watershed or changes in the riverbed configuration due to channel migration. Alternatively, sedimentation may have been halted by a lowering in relative sea level related to climate (e.g., Siddall et al. 2003) or local rebound effects associated with post-glacial isostatic adjustment (Peltier 1998). The timing of renewed sedimentation on the marginal flats of the Tappan Zee at ~1,800–2,500 cal. years B.P. is consistent with the timing of a transgressive event documented within Delaware Bay and Connecticut salt marshes (van de Plassche 1991; Fletcher et al. 1993). This correlation suggests an origin due to regional factors, such as small-scale fluctuations in sea level, rather than local estuarine processes. Because of the shallow water depths and likely role of benthic wave activity in controlling deposition on the Hudson marginal flats, they may contain a stratigraphic record that is especially sensitive to fluctuations in relative sea level.

Fluctuations in oyster presence and Holocene climate variability

The close association between sediment lithofacies and oyster shell documented in our sediment cores indicates that fluctuations in oyster presence in the Hudson estuary during the Holocene has been controlled by changing environmental conditions within the river. Comparison of shell ages with paleoclimate data for the mid- to late Holocene reveals temporal correlations, which suggest that environmental conditions related to climate may have played an important role in the faunal changes observed (Fig. 8). For example, the giant oyster horizon of the shell middens and the basal oysters within our cores coincide with the mid-Holocene warm period known as the Hypsithermal or Holocene Climatic

Optimum when summertime temperatures were 2–4 °C warmer than today (e.g., Webb et al. 1993; Ganopolski et al. 1998). Glacier reconstructions (e.g., Nesje and Kvalme 1991) and ice core data from Greenland and Peru (Larsen et al. 1995; Thompson et al. 1995) indicate the Hypsithermal represented a sustained period (several millennia) of warmer temperatures within the mid-Holocene.

Climate proxies on both a regional and global scale indicate a shift to cooler temperatures at ~4,000–5,000 cal. years B.P. coincident with the onset of the Tappan Zee oyster hiatus (Fig. 8C). In sediments of the New York State Finger Lakes, a decrease in carbonate content and fossil counts occurs at ~3,400–4,500 ^{14}C years (~3,600–5,200 cal. years B.P.), attributed to cooler temperatures following the Hypsithermal (Mullins 1998). Pollen records from the Hudson Highlands indicate a transition to cooler and wetter conditions ca. 4,000 cal. years B.P. (Maenza-Gmelch 1997). On a more global scale, climatic indicators across the North Atlantic, including high-resolution proxy records from SW Ireland and the Sargasso Sea, Bermuda Rise, indicate onset of cooler conditions at 4,600 cal. years B.P., and a return to warmer temperatures by 3,000 cal. years B.P. associated with the Roman and Medieval warm periods (Keigwin 1996; McDermott et al. 2001, Fig. 8C). These warmer periods coincide with the return of oysters in the Tappan Zee.

Similar aged fluctuations in oyster presence are observed within shell middens elsewhere along the Atlantic seaboard (Fig. 8B), providing further support for climatic control. In Georgia and South Carolina, oysters are absent from shell middens between ~2,500 and 4,200 cal. years B.P., and in Florida and North Carolina oysters appear as the dominant shellfish species within local shell middens only after 1,500–2,500 cal. years B.P. (Clasen 1986). Within Maine, oyster shells from the large, Damariscotta River middens have a limited age range of 1,000–2,400 cal. years B.P. (Sanger and Sanger 1986), but older oyster shells (4,100–5,500 cal. years B.P.) have been recovered from Damariscotta River bioherms (Belknap et al. 1994).

Although these correlations along the Atlantic coast are subject to significant age uncertainties associated with reservoir corrections and sparse sampling, the lack of oysters at shell midden sites from Maine to Florida during the cool period ~2,500–4,000 cal. years B.P. following the Hypsithermal is intriguing. The primary environmental factors that influence oyster growth include salinity, temperature, substrate type, and sedimentation rate. The mature oyster can tolerate wide ranges in temperature and salinity. During juvenile development, however, a more limited range of temperatures (20–30 °C) and salinities of 14–25 ppt are optimal (Kennedy et al. 1996). Higher salinities enhance predation and disease, and prolonged periods of freezing temperatures or low salinity associated with freshwater floods cause mortality (Galtsoff 1964; Kennedy et al. 1996). Oysters are also susceptible to high sediment flux

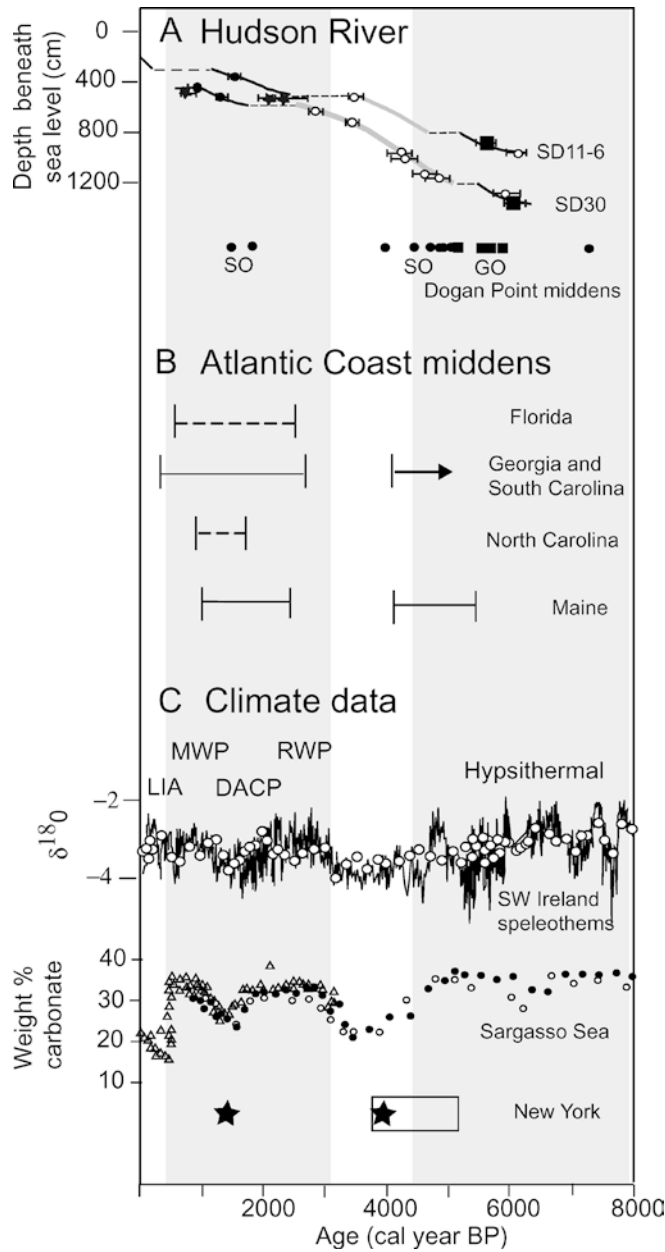


Fig. 8A–C Comparative chronology for the Hudson River, Atlantic coast shell middens, and climate change in and around the North Atlantic. **A** Age-depth data for Hudson River cores from Fig. 7 (see Fig. 7 for definition of symbols/lines). *GO* and *SO* are the dated giant and small oysters, respectively, from Dogan Point middens. Dogan Point shell dates are taken from Little (1995), reservoir-corrected using the same value applied to the river shells and calibrated with CALIB 4.3. **B** Overview of oyster chronology within middens along the Atlantic coast. Age ranges correspond with where oysters are present (*solid lines*) or the dominant species (*dashed line*) within middens. Data for Maine are from Sanger and Sanger (1986) and Belknap et al. (1994). Other data are from Claassen (1986). **C** Climate proxy data for mid- to late Holocene. High-resolution $\delta^{18}\text{O}$ record from SW Ireland speleothems (from McDermott et al. 2001; *open circles* correspond with conventionally sampled and analyzed $\delta^{18}\text{O}$ data, *solid line* corresponds with laser ablation data; *RWP* Roman Warm Period, *DACP* Dark Ages Cold Period, *MWP* Medieval Warm Period, *LIA* Little Ice Age). Weight% carbonate record from Sargasso Sea (from Keigwin 1996; symbols correspond with data from three different cores as described in original source). Local climate data are from the Hudson Valley (*closed stars* denote cooler/wetter conditions, from Maenza-Gmelch 1997) and the Finger Lakes, NY (*rectangle* denotes age range of onset of cooler conditions inferred from lake sediments; Mullins 1998). Grey tone highlights warm periods identified from the high-resolution climate data, which correspond well with phases of oyster presence along the Atlantic seaboard. For data reported in ^{14}C years within source publications (New York and Maine), we apply a standard marine reservoir correction of 400 years for oyster shell, and ages are calibrated using CALIB 4.3 (Stuvier et al. 1998, 2001)

Hypsithermal age (17–23 ppt; Pekar et al. 2004), and more favorable growth conditions associated with higher salinities and warmer water temperatures may account for the larger shells characteristic of this period (i.e., the giant oyster horizon in local shell middens and the large basal oysters in our cores). Sediment samples reveal increased sedimentation rates during the oyster hiatus and higher magnetic susceptibilities, which may reflect an increase in the influx of terrigenous sediments. Local paleoclimate data suggest both cooler and wetter conditions during the period following the Hypsithermal (Maenza-Gmelch 1997). Enhanced stream runoff associated with wetter conditions may have contributed to the higher sediment accumulation rates, along with effects of rising sea level discussed above. Paleowater depths at our core locations have varied from 6–4 m at SD30 to ~2 m at SD11, with oysters present at this full depth range (Fig. 7), and there is no indication that changes in water depth have limited oyster presence within the Tappan Zee.

Based on these paleo-environmental indicators, we speculate that cooler spring and summertime water temperatures during juvenile development, and possibly higher sedimentation rates gave rise to the demise of oysters within the Tappan Zee between 2,500 and 4,000 cal. years B.P. When actively depositing, the clayey silts characteristic of all lithofacies observed within our cores would provide a poor substrate for oyster recruitment (Kennedy et al. 1996). However, the period of non-deposition or erosion marking the boundary between lithofacies 1 and 2 may have played an important role in the return of oysters to the region after

that buries hard substrates necessary for successful spat settlement. Physical disturbance of oyster beds during storms and hurricanes or by winter ice rafting can also cause mortality and limit recruitment.

Paleo-environmental indicators derived from our sediment cores provide constraints on local conditions associated with oyster fluctuations within the Tappan Zee study area. Pekar et al. (2004) use analyses of Foraminifera assemblages and oxygen isotopes from cores SD30 and SD11 to estimate paleosalinities within the region. This study indicates that throughout the past 6,100 years, salinities have remained higher than 10–15 ppt, which is within the range required to support oysters. Based on these data, salinity does not appear to have been a limiting factor for oysters in the region. The highest paleosalinities are derived for sediments of

~2,500 cal. years B.P., by providing a hard substrate more suitable for oyster settlement and development.

Alternate explanations for the oyster demise within the Tappan Zee include devastation by disease or changes in environmental conditions related to the local history of sea-level rise. Widespread mortality due to disease (Dermo and MSX most prevalent, e.g., Kennedy et al. 1996) has affected oyster populations along the Atlantic coast during the past century, and similar massive die-offs may have occurred in the past. Diseased oysters may experience growth inhibition, and analysis of fossil oyster shells within Tappan Zee sediments could help elucidate any linkage with disease or predators.

Post-glacial sea-level rise has contributed to the sedimentary history of the Tappan Zee (e.g., Newman et al. 1969; Weiss 1974; McHugh et al. 2004) and could also contribute to the observed faunal changes, as they relate to sedimentation rates and salinity. As discussed above, the paleosalinity data of Pekar et al. (2004) indicate salinities within the region adequate to support oysters throughout the mid- to late Holocene. Higher rates of sediment accumulation during the oyster hiatus may have played an important role in inhibiting oyster colonization, and are plausibly related to both climate and sea-level rise. The history of Holocene sea-level movements around the globe reflects glacial isostatic adjustment, as well as eustatic contributions linked to climate through the melting of continental ice sheets, thermal expansion of the oceans, and possible changes in thermohaline circulation (e.g., Peltier 1998). Along the Atlantic coast, isostatic effects are complex, with different responses in magnitude and timing from glacial rebound and water loading (e.g., Tushingham and Peltier 1992). As a result, isostatic sea-level movements are not as likely to be synchronous and in phase as the forcing from climate change. Based on the temporal correlations between oyster presence and climate proxies evident in the existing data from along the Atlantic coast, we favor climatic control. However, confirmation of this hypothesis will clearly require further studies of paleo-environmental indicators, including high-resolution sea-level observations both within the Hudson and in other mesohaline systems along the Atlantic coast where a history of oyster presence is found.

Demise of the Tappan Zee oyster beds within the last millennia

Shell dating from the Dogan Point middens suggests the youngest phase of oyster harvesting by indigenous peoples (oyster shell dates range 1,500–1,800 cal. years B.P.) ceased prior to European contact, although charcoal and other artifacts above the shells indicate occupation up to colonial times (Little 1995; Claassen 1995). The youngest oyster shell ages (500–900 cal. years B.P.) recovered from the Tappan Zee sediments also suggest that oysters failed again within the last millennium. Although reports from early settlers indicate that they were aware of oyster beds within the Tappan Zee (Ingersoll 1881), to our knowledge

significant commercial harvesting did not occur in this area during colonial times. In the 1950s oyster cultivators briefly used the Tappan Zee beds as nursery beds (Bromley 1954). Although over-harvesting of the Tappan Zee beds by non-commercial colonial activity cannot be ruled out, our existing shell dates suggest a major demise at ~500–900 years B.P. (Fig. 8). This timing is consistent with the onset of the Little Ice Age, a period of increased storm activity within the northeastern US (Noren et al. 2002), and lower temperatures with more severe winters during which glaciers in many parts of the globe expanded (Grove 1988). Within Chesapeake Bay, Cronin et al. (2003) report a sustained period of cooler springtime water temperatures (by ~2–5°C) during the Little Ice Age relative to the earlier Medieval Warm Period. Similar cool spring and summer water temperatures within the Hudson at this time may have negatively impacted oyster growth, particularly during the juvenile phase of development. Physical damage to oyster beds from ice rafting or frequent storm events could also have been important in the demise of the Tappan Zee oyster population. Indeed, the oyster bed remnants documented within the Tappan Zee channel in the present study indicate significant erosion of the shallowest beds has occurred in the recent past. Dates from shell middens elsewhere along the Atlantic coast also suggest an end in widespread indigenous oyster harvesting prior to colonization, and changing climatic conditions associated with the Little Ice Age may have impacted oyster populations within estuaries throughout the region (Fig. 8).

Modern salinities within the Tappan Zee (summer range of ~10–13 ppt) are at the lower limit of the required range for oysters, and we anticipate that oyster beds within this marginal environment are more vulnerable to effects of climate changes than beds closer to the ocean. For example, within the higher-salinity conditions of New York Harbor, a robust oyster industry thrived throughout colonial times until the early 1900s when over-harvesting, pollution, and market forces caused the industry to close down (MacKenzie 1996). Elsewhere along the Atlantic coast, many of the shell middens where temporal fluctuations in oyster presence are observed are located at upriver sites (Claassen 1986) where local oyster beds may have developed at the limits of their environmental range during favorable climatic conditions, serving as sensitive indicators of climatic shifts through time. With post-Little Ice Age warming in the northern Atlantic region, efforts to restore estuarine oyster populations along the east coast may be well timed. Indeed, during our sampling, young live oysters were occasionally recovered within the Tappan Zee. A natural restoration may already be underway.

Conclusions

Our study of geophysical and sampling data reveals fossil oyster beds within the marginal flats of the mesohaline Hudson River estuary. Shell ages and changes in

valve size match those found in local shell middens, and the fossil beds likely represent those harvested by local indigenous peoples up to >6,000 cal. years b.p. The available age control indicates oysters thrived within two distinct warm periods during the Holocene—the mid-Holocene hypsithermal ending ~4,000 cal. years b.p., and the Roman and Medieval warm periods beginning ~2,500 cal. years b.p. Oysters disappeared from the region during the intervening period of cooler conditions, and with onset of the Little Ice Age. Similar age fluctuations in oyster presence are evident in local shell midden sites elsewhere along the Atlantic coast, and may reflect the sensitivity of oysters in marginal upstream mesohaline settings to climate fluctuations. Although anthropogenic impacts appear to dominate modern estuarine ecosystems, these impacts occur within the context of naturally changing environmental conditions, which must be understood if restoration and mitigation programs targeted at modern degraded estuaries are to be effective.

Acknowledgements Our research was supported by the Hudson River Foundation for Science and Environmental Research Inc. under grant 003/00A to SMC and REB, and the New York State Department of Environmental Conservation that provided funding for the primary data collection from the Environmental Protection Fund through the Hudson River Estuary Program. We thank D. Strayer, J. Bratton, D. Belknap, P. Vogt and R. McBride for their comments, which improved the manuscript. We are greatly indebted to E. Blair and J. Ladd for their ongoing enthusiastic support of this work. We thank Captain John Lipscomb, Riverkeeper, and the captain and crew of the *L.F. Walford*, New Jersey Marine Consortium, for excellent support during survey operations. Orange and Rockland County Gas and Electric generously provided access to their vibracores and supported acquisition of SD30 for scientific goals. We thank Tom Guilderson of Lawrence Livermore National Labs and Irka Hajdas of the Radiocarbon Laboratory, University of Zurich for radiocarbon analyses. Nicole Anest of the Lamont-Doherty Earth Observatory Deep-Sea Sample Repository carried out physical property analyses. Support for the collection and curating facilities of the LDEO core repository, where all sample material used in this study is archived, is provided by the National Science Foundation (grant OCE00-02380) and the Office of Naval Research (grant N00014-02-1-0073). Lamont-Doherty Earth Observatory contribution #6595.

References

- Baucom PC, Bratton JF, Colman SM, Moore J, King J, Heil C, Seal R (2001) Selected data for sediment cores collected in Chesapeake Bay in 1996 and 1998. USGS Open-File Rep 01-194
- Belknap DF, Kraft JC, Dunn RK (1994) Transgressive valley-fill lithosomes: Delaware and Maine. In: Incised-valley systems: origin and sedimentary sequences. SEPM Spec Publ 51:303–320
- Bell RE, Flood RD, Carbotte SM, Ryan WBF, McHugh C, Cormier M-H, Versteeg R, Chayes D, Bokuniewicz H, Ferrini V, Thissen J (2000) Hudson River Estuary Program Benthic Mapping Project. Final Report to New York State Department of Environmental Conservation
- Bell RE, Flood RD, Carbotte SM, Ryan WBF, Nitsche FO, Chirlrud S, Arko R, Ferrini V, Slagle A, Bertinato C, Turrin M (2003) Hudson River Estuary Program Benthic Mapping Project. New York State Department of Environmental Conservation Phase II, Rep 1
- Bratton JF, Colman SM, Thieler ER, Seal RR II (2003) Birth of the modern Chesapeake Bay estuary 7,400 to 8,200 years ago and implications for global sea-level rise. *Geo-Mar Lett* 22:188–197
- Brennan LA (1974) The lower Hudson: a decade of shell middens. *Archaeol Eastern North Am* 2(1):81–93
- Bromley A (1954) The Oyster and the Brothers Flower: the Hudson River and private enterprise combine to write a new story. *New York State Conservationist*:4–9
- Claassen C (1986) Temporal patterns in marine shellfish-species use along the Atlantic coast in the southeastern United States. *Southeastern Archaeol* 5:120–137
- Claassen C (1995) Dogan Point and its social context. In: Claassen C (ed) Dogan Point: a shell matrix site in the lower Hudson Valley. Occasional Publ Northeastern Anthropol 14:129–142
- Colman SM, Baucom PC, Bratton JF, Cronin TM, McGeehin JP, Willard D, Zimmerman AR, Vogt P (2002) Radiocarbon dating, chronological framework, and changes in accumulation rates of Holocene estuarine sediments from Chesapeake Bay. *Quat Res* 57:58–79
- Cronin TM, Dwyer GS, Kamiya T, Schwede S, Willard DA (2003) Medieval warm period, Little Ice Age and 20th century temperature variability from Chesapeake Bay. *Global Planet Change* 36:17–29
- Fletcher CH III, Pizzuto JE, Suku J, van Pelt JE (1993) Sea-level rise acceleration and the drowning of the Delaware Bay coast at 1.8 ka. *Geology* 21:121–124
- Galtsoff PS (1964) The American oyster: *Crassostrea virginica* [Gmelin]. US Fish Wildlife Service, Washington, US, Fish Bull 64
- Ganopolski A, Kubatzki C, Claussen M, Brovkin V, Petoukhov V (1998) The influence of vegetation-atmosphere-ocean interaction on climate during the mid-Holocene. *Science* 280:1916–1919
- Grove JM (1988) The Little Ice Age. Methuen, London
- Hagen RA, Vogt PR (1999) Seasonal variability of shallow biogenic gas in Chesapeake Bay. *Mar Geol* 158:75–88
- Hill JM, Halka JP, Conkwright R, Koczot K, Colman SM (1992) Distribution and effects of shallow gas on bulk estuarine sediment processes. *Cont Shelf Res* 12:1219–1229
- Ingersoll E (1881) The oyster industry. In: Goode GB (ed) The history and present condition of the fishery industries. Tenth Census United States, US Department of the Interior, Washington, DC, pp 1–252
- Jackson JBC, 18 others (2001) Historical overfishing and the recent collapse of coastal ecosystems. *Science* 293:629–638
- Keigwin LD (1996) The little ice age and medieval warm period in the Sargasso Sea. *Science* 274:1503–1508
- Kennedy VS, Newell RI, Eble AF (1996) The Eastern Oyster. Maryland Sea Grant College, College Park, Maryland
- Larsen E, Sejrup HP, Johnsen SJ, Knudsen KL (1995) Do Greenland ice cores reflect NW European interglacial climate variations? *Quat Res* 43:125–132
- Little E (1995) Apples and oranges: radiocarbon dates on shell and charcoal at Dogan Point. In: Claassen C (ed) Dogan Point: a shell matrix site in the lower Hudson Valley. Occasional Publ Northeastern Anthropol 14:121–128
- MacKenzie CL Jr (1996) History of oystering in the United States and Canada, featuring the eight greatest oyster estuaries. *Mar Fish Rev* 58:1–78
- Maenza-Gmelch T (1997) Holocene vegetation, climate, and fire history of the Hudson Highlands, southeastern New York, USA. *Holocene* 7:25–37
- McDermott F, Matthey DP, Hawkesworth C (2001) Centennial-scale Holocene climate variability revealed by a high-resolution speleothem $\delta^{18}\text{O}$ record from SW Ireland. *Science* 294:1328–1331
- McHugh CMG, Pekar S, Christie-Blick N, Ryan WBF, Carbotte SM, Bell RE (2004) Spatial variations in a condensed interval between estuarine and open marine settings: Holocene Hudson River estuary and adjacent continental shelf. *Geology* 32:168–172

- Mullins HT (1998) Holocene lake level and climate change inferred from marl stratigraphy of the Cayuga lake basin, New York. *J Sediment Res* 68:569–578
- Nesje A, Kvamme M (1991) Holocene glacier and climate variation in western Norway: evidence for early Holocene glacier demise and multiple neoglacial events. *Geology* 19:610–612
- Newman WS, Thurber DH, Zeiss HS, Rokach A, Musich L (1969) Late Quaternary geology of the Hudson River estuary: a preliminary report. *New York Acad Sci Trans Ser II* 31:548–570
- NOAA (2000) Benthic habitats of selected areas of the Hudson River, NY based on sediment profile imagery. Coastal Services Center Report to NYSDEC
- Noren AJ, Bierman PR, Steig EJ, Lini A, Southon J (2002) Millennial-scale storminess variability in the northeastern United States during the Holocene epoch. *Nature* 419:821–824
- Olson CB, Simpson HJ, Bopp RF, Wiliams SC, Peng TH, Deck BL (1978) A geochemical analysis of the sediments and sedimentation in the Hudson Estuary. *J Sediment Petrol* 48:401–418
- Pekar SF, McHugh CM, Christie-Blick N, Jones M, Carbotte SM, Bell RE (2004) Estuarine processes and their stratigraphic record: paleosalinity and sedimentation changes in the Hudson Estuary. *Mar Geol* (in press)
- Peltier WR (1998) Postglacial variations in the level of the sea: implications for climate dynamics and solid-earth geophysics. *Rev Geophys* 36:603–689
- Peltier WR (1999) Global sea level rise and glacial isostatic adjustment. *Global Planet Change* 20:93–123
- Sanford LP (1994) Wave-forced resuspension of upper Chesapeake Bay muds. *Estuaries* 17:148–165
- Sanger D, Sanger MJ (1986) Boom and bust on the river: the story of the Damariscotta oyster shell heaps. *Archaeol Eastern North Am* 14:65–78
- Schock S, Leblanc LR (1990) Chirp sonar; new technology for subbottom. *Sea Technol* 31:35–43
- Schuldenrein J (1995) Prehistory and the changing Holocene geography of Dogan Point. In: Claassen C (ed) Dogan Point: a shell matrix site in the lower Hudson Valley. Occasional Publ Northeastern Anthropol 14:39–64
- Siddall M, Rohling EJ, Almogi-Labin A, Hemleben C, Meischner D, Schmeizer I, Smeed DA (2003) Sea-level fluctuations during the last glacial cycle. *Nature* 423:853–858
- Smith GF, Roach EB, Bruce DG (2003) The location, composition, and origin of oyster bars in mesohaline Chesapeake Bay. *Estuarine Coastal Shelf Sci* 56:391–409
- Stuiver M, Reimer PJ, Bard E, Beck JW, Burr GS, Hughen KA, Krommer B, McCormac FG, Plicht JVD, Spurk M (1998) INTCAL98 radiocarbon age calibration, 24,000–0 cal BP. *Radiocarbon* 40:1041–1083
- Stuiver M, Reimer PJ, Reimer R (2001) CALIB radiocarbon calibration, HTML version 4.3. University of Washington <http://calib.org/calib/>
- Thompson LG, Mosley-Thompson E, Davis ME, Lin PN, Henderson KA, Cole-Dai J, Bolzan JF, Liu KB (1995) Late glacial stage and Holocene tropical ice core records from Huascarán, Peru. *Science* 269:46–50
- Tushingham AM, Peltier WR (1992) Validation of the ICE-3G Model of Wurm-Wisconsin Deglaciation using a global data base of relative sea level histories. *J Geophys Res* 97:3285–3304
- van de Plassche O (1991) Late Holocene sea-level fluctuations on the shore of Connecticut inferred from transgressive and regressive overlap boundaries in salt-marsh deposits. *J Coastal Res Spec Issue* 11:159–179
- Walther GR, Post E, Convey P, Menzel A, Parmesan C, Beebee TJC, Fromentin J-M, Hoegh-Guldberg O, Bairlein F (2002) Ecological responses to recent climate change. *Nature* 416:389–395
- Webb T III, Bartlein PJ, Harrison SP, Anderson KH (1993) Vegetation, lake levels, and climate in eastern North America for the past 18000 years. In: Wright HE, Kutzbach JE, Webb T III, Ruddiman WF, Street-Perrott FA, Bartlein PJ (eds) *Global climates since the last Glacial Maximum*. University of Minnesota Press, Minneapolis, MN, pp 415–467
- Weiss D (1974) Late Pleistocene stratigraphy and paleoecology of the lower Hudson River estuary. *Geol Soc Am Bull* 85:1561–1570